

Selectivity in the Addition Reactions of Organometallic Reagents to Aziridine-2-carboxaldehydes: The Effects of Protecting Groups and Substitution Patterns

Aman Kulshrestha,^[a] Jennifer M. Schomaker,^[b] Daniel Holmes,^[a] Richard J. Staples,^[a] James E. Jackson,^{*[a]} and Babak Borhan^{*[a]}

Abstract: Good to excellent stereo-selectivity has been found in the addition reactions of Grignard and organozinc reagents to N-protected aziridine-2-carboxaldehydes. Specifically, high *syn* selectivity was obtained with benzyl-protected *cis*, *tert*-butyloxycarbonyl-protected *trans*, and tosyl-protected 2,3-disubstituted aziridine-2-carboxaldehydes. Furthermore, rate and selectivity effects of ring substituents, temperature, solvent, and Lewis acid

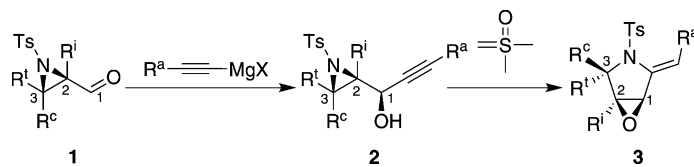
and base modifiers were studied. The diastereomeric preference of addition is dominated by the substrate aziridines' substitution pattern and especially the electronic character and con-

formational preferences of the nitrogen protecting groups. To help rationalize the observed stereochemical outcomes, conformational and electronic structural analyses of a series of model systems representing the various substitution patterns have been explored by density functional calculations at the B3LYP/6-31G* level of theory with the SM8 solvation model to account for solvent effects.

Keywords: aziridines • conformation analysis • density functional calculations • Grignard reaction • invertomers • stereochemistry • substituent effects

Introduction

Aziridines are important subunits in chiral auxiliaries, pharmaceutical intermediates, and biologically active natural products.^[1] Available through several recently developed stereo- and enantioselective syntheses,^[1c,2] these compact and robust heterocycles are endowed with controllable reactivity due to their three-membered-ring strain and their amine site's acid- and substituent-governed activation. Thus, through modern regio- and stereoselective ring-opening methods, aziridine building blocks offer efficient, versatile access to structurally complex targets. For example, we have recently reported that *N*-tosyl-2,3-disubstituted aziridine-2-carboxaldehydes (**1**) undergo addition reactions with Grignard reagents to form *syn* adducts **2** ($R^i = \text{CH}_3$, $R^t = \text{alkyl}$, $R^c = \text{H}$) with excellent diastereoselectivity ($>99:1$; Scheme 1). The use of these products as starting materials



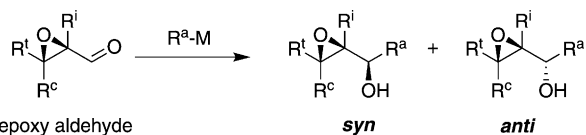
Scheme 1. Ts-protected aziridine carboxaldehydes serve as precursors for the tandem aza-Payne/hydroamination methodology.

enabled our discovery of a one-pot tandem aza-Payne/hydroamination reaction, a process that yields highly functionalized, densely substituted pyrrolidines **3** (Scheme 1).^[3] Notably, it is the newly generated carbinol stereocenter that is the key to the success of these reactions.

This report explores the elaboration of aziridine-2-carboxaldehydes through nucleophilic carbonyl addition reactions that install a stereocenter adjacent to and guided by the rigid, stereochemically defined aziridine ring. With three consecutive stereocenters, the resulting aziridinyl carbinols are poised for application in a wide range of synthetic transformations.^[3–4] Such chemistry has proven useful with epoxides, the oxygen-containing analogues of aziridines; the addition reactions of organometallic reagents to α,β -epoxy aldehydes have been extensively studied and exploited in the syntheses of natural products.^[5] These additions (Scheme 2) form a new stereogenic center, giving rise to either *syn* or *anti* adducts depending on the choice of metal. Those that are strong coordinators favor *syn* selectivity, which can be rationalized by a chelation-based transition-state model.^[5b]

[a] Dr. A. Kulshrestha, Dr. D. Holmes, Dr. R. J. Staples, Prof. J. E. Jackson, Prof. B. Borhan
Department of Chemistry, Michigan State University
East Lansing, MI 48824 (USA)
Fax: (+1) 517-353-1793
E-mail: jackson@chemistry.msu.edu
babak@chemistry.msu.edu

[b] J. M. Schomaker
Department of Chemistry, University of Wisconsin
1101 University Avenue, Madison, WI 53706 (USA)
Supporting information for this article is available on the WWW under <http://dx.doi.org/10.1002/chem.201101168>.



Scheme 2. The addition of organometallic reagents to epoxy aldehydes. R^c, Rⁱ, and R^a represent substituents that are *cis*, *trans*, or *ipso* to the aldehyde, respectively. R^a denotes the nucleophile added to the carbonyl.

On the other hand, metals that coordinate poorly or conditions that suppress chelation favor the *anti* adduct predicted by the Felkin–Anh model.^[6] The substitution pattern in the starting material also influences the *syn/anti* selectivity, the effects of which are understood for α,β -epoxy aldehydes.^[5b] Aziridine-2-carboxaldehydes, however, gain additional electronic and steric degrees of freedom from the nitrogen's pyramidal geometry and substituent variability.

A limited number of other reports have explored the reactions of organometallic reagents with aziridine carbonyl species. Addition of boron enolates to *N*-*tert*-butyloxycarbonyl (*N*-Boc) *trans*-substituted aziridine-2-carboxaldehydes proceeds with high *anti* selectivity.^[4c] Reductions of aziridine ketones with various reagents have led to similar results, that is, the nucleophile attacks by the *pro-anti* approach.^[7] In both cases, the stereochemical outcomes were rationalized in terms of Felkin–Anh transition states for attack on the carbonyl site (Scheme 3a). It should be noted, however, that the latter precedent is not universally applicable; the *pro-syn* approach can dominate under some conditions.^[8]

Investigating the addition of Grignard reagents to *N*-Boc-protected aziridine-2-carboxaldehydes, Righi and co-workers

reported excellent *syn* selectivity with *trans* substrates, a result they attributed to N-centered chelation control (Scheme 3b).^[4b] This selectivity was completely lost in the case of *cis* substrates, the cyclic chelate intermediates of which the authors judged to be unfavorably strained. Contrarily, in a related study of benzyl (Bn)-protected aziridine carboxaldehydes,^[4a] Andres and co-workers observed high *syn* selectivity specifically in the case of *cis* substrates and invoked chelation control to justify the selectivity. These two reports appear contradictory; more precisely, taken together, they suggest that chelation control and the resulting product selectivities are a function of both N protecting group and substitution pattern.

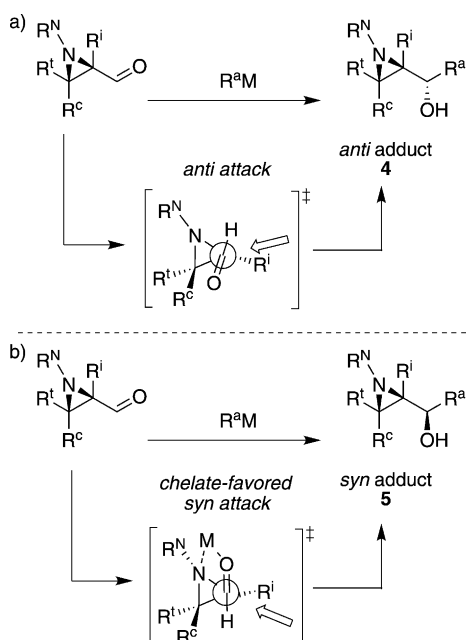
Noting the limited number of studies on stereoselective additions of carbon nucleophiles to aziridine-2-carboxaldehydes, and intrigued by the widely varying diastereoselectivities in our own studies of *N*-tosyl (Ts)-protected systems (Scheme 1), we recognized the need for a set of principles to rationalize observations and guide synthetic decisions. We therefore undertook a combined theoretical and experimental study of nucleophilic reagent additions to *cis*- and *trans*-substituted aziridine-2-carboxaldehydes with various substituents on nitrogen.

To establish a common reference framework, an initial set of detailed quantum chemical studies were carried out on truncated model systems. By exploring the ground-state conformational preferences of the various substitution patterns, our aim was to develop not only useful insights, but also a simple procedure to routinely predict reactions' stereochemical outcomes.

To map the effects of electronic variations at nitrogen on reaction selectivity, we chose the common nitrogen protecting groups: alkyl, alkoxy carbonyl, and alkylsulfonyl. In the abbreviated models used to simplify the theoretical analysis, these were methyl (Me), methoxycarbonyl (Moc), and methanesulfonyl (Ms) groups; the corresponding experimental systems employed Bn, Boc and Ts groups. A simple alkyl or Bn group leaves the nitrogen comparatively electron rich and amine-like; Boc's moderate ability as a π -acceptor and strong conformational preferences offer intermediate activation; Ts is the most electron-withdrawing group but is less conformationally defined than Boc. The results of our study provide intuitive insight and a working model for controlling the selective addition of organometallic reagents to aziridine-2-carboxaldehydes. The unique combinations of nitrogen protecting groups and aziridine substitution patterns that yield the highest stereoselectivity are identified; interestingly, these are different for each of the protecting groups.

Results and Discussion

To develop an understanding of the relevant conformational preferences and to set the stage for analysis of experimental results, fifteen model substituted aziridine-2-carboxaldehydes were studied by quantum chemical modeling. Specifi-



Scheme 3. a) The Felkin–Anh model. b) The Chelation-control model. The N-bound substituent is denoted R^N; see Scheme 2 for details of the other labels.

cally, 1) gas-phase DFT simulations of substrates' ground-state conformations were run in the hope that the preferences uncovered would offer simple explanations for the experimental stereochemical outcomes; 2) solvation effects of the CH_2Cl_2 reaction medium were simulated through single point SM8 calculations on the minima computed; 3) the validity of the gas-phase DFT energetic analyses was verified through comparison of a subset of the systems studied with G3(MP2) composite thermochemistry calculations; and 4) selected potential-energy functions for aldehyde rotation and nitrogen inversion were also explored in several model aziridine-2-carboxaldehydes.

All calculations were performed with the Spartan 08^[9] software package, by using the B3LYP functional,^[10] the 6-31G* basis set,^[11] and the SM8 solvation modeling scheme^[12] to account for the effects of the CH_2Cl_2 solvent environment. To check the performance of this DFT-based method, the G3(MP2) composite scheme was used; this method offers near-experimental accuracy for the heats of formation and reaction energetics of small gas-phase organic molecules.^[13]

Conformational analysis of ground state aziridine-2-carboxaldehydes: The model systems considered are shown in Table 1, together with energetic information on their preferred conformations and the energy gap (in kcal mol^{-1}) that separates each compound's lowest energy minimum from its

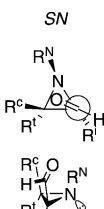
Table 1. Conformer energies of modeled aziridine-2-carboxaldehydes.

Name	R^{N}	R^{i}	R^{t}	R^{c}	Lowest $E^{[\text{a}]}$ conformer	$\Delta E^{[\text{a}]}$ to 2nd lowest $E^{[\text{a}]}$ conformer	2nd lowest $E^{[\text{a}]}$ conformer	Conformer			
								AX	SX	AN	SN
Me-H3	CH_3	H	H	H	AX	1.42	AN	0.00	2.60	1.42	2.53
Me-ipso	CH_3	CH_3	H	H	AX	0.44	SX	0.00	0.44	2.59	0.95
Me-trans	CH_3	H	CH_3	H	SN	0.30	AX	0.30	0.31	1.66	0.00
Me-cis	CH_3	H	H	CH_3	AX	0.48	AN	0.00	5.47	0.48	4.03
Me-2,3Di	CH_3	CH_3	CH_3	H	SX	0.19	SN	1.80	0.00	4.22	0.19
Moc-H3	CO_2CH_3	H	H	H	SN	0.53	AX	0.53	0.93	1.76	0.00
Moc-ipso	CO_2CH_3	CH_3	H	H	SX	0.01	SN	0.28	0.00	2.37	0.01
Moc-trans	CO_2CH_3	H	CH_3	H	$\text{SN}^{[\text{c}]}$	1.20	SX	1.32	1.20	2.32	0.00
Moc-cis	CO_2CH_3	H	H	CH_3	AX	0.21	AN	0.00	1.77	0.21	0.26
Moc-2,3Di	CO_2CH_3	CH_3	CH_3	H	SN	0.23	SX	1.97	0.23	3.69	0.00
Ms-H3	SO_2CH_3	H	H	H	AX	1.30	AN	0.00	2.06	1.30	4.72
Ms-ipso	SO_2CH_3	CH_3	H	H	SX	0.18	AX	0.18	0.00	2.23	3.35
Ms-trans	SO_2CH_3	H	CH_3	H	SX	0.50	AX	0.50	0.00	1.37	2.45
Ms-cis	SO_2CH_3	H	H	CH_3	AX	0.42	AN	0.00	5.84	0.42	6.66
Ms-2,3Di	SO_2CH_3	CH_3	CH_3	H	$\text{SX}^{[\text{d}]}$	3.14	SN	4.03	0.00	5.95	3.14

[a] All energies shown in kcal mol^{-1} ; [b] AX , SX , AN , and SN label the conformers as *anti* or *syn* (relationship of R^{N} to CHO) and *exo* or *endo* (orientation of the CHO group relative to the aziridine ring); [c] An SN conformation like that here in **Moc-trans** is seen in the X-ray crystal structure of the related *trans* N-Boc analogue **8** (see below); [d] An SX conformation like that in **Ms-2,3Di** is seen in the X-ray crystal structure of related *trans* N-Ts-2,3-disubstituted 2-carboxaldehyde analogue **15**.

next lowest energy conformation of a different category. Two binary choices define the four categories of conformations listed; these are 1) the relationship (*anti* or *syn*) between the N substituent (R^{N}) and the aldehyde moiety; and 2) the rotamer orientation of the aldehyde carbonyl oxygen, that is, *exo*, with the hydrogen over the ring, or *endo*, with the oxygen over the ring. This choice deserves comment here; the conjugation of carbonyl groups with adjacent cyclopropyl rings in the bisected *endo* (*s-cis*) and *exo* (*s-trans*) conformations has long been known (Figure 1a).^[14] Like cyclopropane, the aziridine ring favors bisected conformations for attached carbonyl groups, leading to this simple *exo/endo* choice. This conjugative preference is surprisingly insensitive to the replacement of carbon with a heteroatom, in terms of preferred rotameric angle.^[15] The $\tau\text{H}^1\text{CCH}^{\text{CHO}}$ (for which H^1 is analogous to R^{i} in Table 1) dihedral angle values deviate only by $\pm 15^\circ$ relative to the 0° and 180° seen in cyclopropane carboxaldehyde. Nucleophilic addition reactions to cyclopropyl carbonyl compounds have also been systematically investigated^[16] and often show selectivity governed by the more stable bisected conformation.^[16a,17]

The aforementioned conformational choices are coded *A* versus *S* (*anti* vs. *syn*), and *X* versus *N* (*exo* vs. *endo*), respectively, leading to the four categories *AX*, *AN*, *SX*, and *SN*. If more than four conformers exist due to R^{N} rotation, the energies listed in the table represent the lowest energy conformer in each category.



As noted above, the model R^{N} groups CH_3 , COOCH_3 , and SO_2CH_3 were chosen to simulate *Bn*, *Boc*, and *Ts* substituents, respectively. Even without inspecting the full conformer list, including R^{N} rotamers, it is immediately evident that relatively few of the model substrates considered here have a strong structural bias toward a particular conformation. However, it is noteworthy that the structures calculated to be most conformationally defined correspond to analogues with strong experimental stereoselectivities. Also, in cases for which *AN* is low enough in relative energy, this conformation allows for chelation to exert further directing effects with Grignard and organozinc nucleophiles.

Before delving into the significance of the conformational findings in Table 1, several checks on the appropriateness of this level of calculation should be discussed. The $1.42 \text{ kcal mol}^{-1}$ *AX* preference

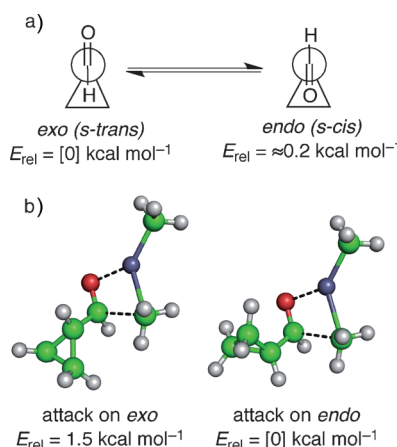


Figure 1. a) Bisected *exo* (*s*-*trans*) and *endo* (*s*-*cis*) conformations of cyclopropyl carbonyl systems. b) B3LYP/6-31+G* optimized TS structures (relative energies with vibrational, thermal, and solvent corrections) for attack of $(\text{CH}_3)_2\text{Zn}$ on *endo* and *exo* conformations of cyclopropane carboxaldehyde.

computed for **Me-H3** is consistent with the conformation assigned to *N*-*tert*-butylaziridine-2-carboxaldehyde by Pierre et al. on the basis of variations in the H-C-C(=O)-H ^1H NMR coupling constant with temperature and solvent polarity.^[18] Likewise, the small energy differences calculated for **Me-trans** conformations are consistent both with the invertomer distribution of 2-acetyl-*N*,*3*-dimethyl aziridine observed previously, and with our own findings for the closely related *trans*-*N*-benzyl-3-ethylaziridine-2-carboxaldehyde **7** discussed below.^[19] As noted in Table 1, X-ray crystal structures of *N*-Boc-*trans*-3-cyclohexylaziridine-2-carboxaldehyde **8** and *N*-Ts-*trans*-3-benzyloxymethyl-2-methylaziridin-2-carboxaldehyde **15**, the experimental analogues of **Moc-trans** and **Ms-2,3Di**, confirm the calculated minimum energy conformational assignments. Broader support is found in the G3(MP2) calculations on the *N*-methyl series of model substrates. As noted above, this level of calculation is designed to provide energetics comparable to experiment in quality. Table 2 compares their “ CH_2Cl_2 solvated” enthalpies as calculated at the DFT and G3(MP2) levels. Although not a perfect match, the energy variations seen in the DFT results generally mirror the G3(MP2) data.

To translate the conformational preferences computed above into predictions regarding the stereochemistry of nucleophilic attack, some estimate of the intrinsic reactivities and stereoselectivities of the *exo* versus *endo* CHO rotamer

conformations must first be made. Then directing effects due to the roles of chelation and sterically interfering substituents can be explored.

Carbonyl conformation: *endo* versus *exo*: Focusing on the steric demands of a carbon nucleophile alone, it might be expected that an *endo*-oriented carboxaldehyde conformer should be more reactive than an *exo* one, as attack along the Bürgi–Dunitz angle would be likely to encounter more interference approaching the *exo* conformer. However, an organometallic compound, such as a Grignard or organozinc reagent, likely follows a less open trajectory as its metal component coordinates to the increasingly negative carbonyl oxygen. Nonetheless, the assumption is supported by B3LYP/6-31+G* calculations on the transition states for dimethylzinc attacking cyclopropane carboxaldehydes (Figure 1 b). Although the substrate’s ground state conformation is found to prefer the *exo* geometry by 0.1–0.2 kcal mol⁻¹ (0.27 experimental),^[20] the *endo* attack transition state (TS) is favored over the *exo* by 1.7 kcal mol⁻¹ (1.5 with vibrational, thermal, and solvation corrections), which is enough to create a $>10:1$ preference for the *endo* path at relevant reaction temperatures. Although further skewed by the aziridine nitrogen’s own chelation and conformational dynamics, this steric bias towards attack on *endo* aldehyde conformations remains true for aziridine-2-carboxaldehydes in which the substituent *ipso* to the aldehyde is hydrogen.

As is evident from Table 1, replacement of the *ipso* hydrogen with an alkyl group in the R^i site has two notable effects on ground-state conformations: 1) it adds steric bulk on the *trans* face which, in turn, decreases the *anti*–*syn* energy gap by shifting the *anti* form up in energy relative to the *syn* invertomers at nitrogen regardless of the nature of R^N ; and 2) it adds a stereoelectronic preference for the *exo* over the *endo* aldehyde rotamer. Although the origin of the latter preference is not analyzed here, the added invertomer bias can be as large as 2–3 kcal mol⁻¹, whereas the aldehyde rotamer preference is in the 0.5–1 kcal mol⁻¹ range. To illustrate, comparison of the **Me-H3** and **Me-ipso** models, both of which have *AX* lowest energy conformers, is instructive: 1) The energy changes for *N*-CH₃ inversion from *syn* to *anti* are shifted to favor the *syn* isomer upon adding the methyl group, that is, on going from **Me-H3** ($\Delta E_{\text{SX} \rightarrow \text{AX}} = -2.60$ and $\Delta E_{\text{SN} \rightarrow \text{AN}} = -1.11$) to **Me-ipso** ($\Delta E_{\text{SX} \rightarrow \text{AX}} = -0.44$ and $\Delta E_{\text{SN} \rightarrow \text{AN}} = +1.64$). Thus, the *ipso* CH₃ group adds 2.16 and 2.75 kcal mol⁻¹, respectively, to the steric cost for the *N*-CH₃ to be on the *trans* face, balancing (but not completely overcoming) the preference for the *anti* forms. Analogous numbers for the Ts model (Ms series) are 2.24 and 2.30 kcal mol⁻¹, which are quite similar to those seen for the Me set; in this case the *anti* preference is overcome, moving SX to the lowest energy spot. Interestingly, the Moc series is only shifted by 0.68 and 0.60 kcal mol⁻¹, which is consistent with Moc’s strong preference (due to N conjugation) for orienting its thinnest dimension towards vicinal substituents. 2) Comparisons analogous to those above, but comparing aldehyde rotamers are shifted as follows: $\Delta E_{\text{AN} \rightarrow \text{AX}} = -1.42$

Table 2. Comparison of the relative energies of B3LYP/6-31G*/SM8 CH_2Cl_2 (DFT) and G3(MP2)/SM8 CH_2Cl_2 (G3).

	<i>AX</i>		<i>SX</i>		<i>AN</i>		<i>SN</i>	
	DFT	G3	DFT	G3	DFT	G3	DFT	G3
Me-H3	0.00	0.00	2.60	2.98	1.42	1.79	2.53	3.54
Me-ipso	0.00	0.00	0.44	0.82	2.59	2.87	0.95	1.89
Me-trans	0.30	0.00	0.31	0.26	1.66	1.80	0.00	0.75
Me-cis	0.00	0.00	5.47	5.56	0.48	0.98	4.03	5.00
Me-2,3Di	1.80	1.32	0.00	0.00	4.22	4.08	0.19	1.01

and $\Delta E_{SN-SX} = +0.07 \text{ kcal mol}^{-1}$ for **Me-H3** versus $\Delta E_{AN-AX} = -2.59$ and $\Delta E_{SN-SX} = -0.51 \text{ kcal mol}^{-1}$ for **Me-ipso**. Thus, the *ipso* CH_3 group favors the *exo* rotamer by 1.17 and 0.58 kcal mol^{-1} , respectively; analogous pairs of values for the Moc and Ms systems are 0.86/0.94 and 0.75/0.69 kcal mol^{-1} .

But what of the transition states? How does addition of an *ipso* alkyl group affect the relative energetics of *endo* versus *exo* attack? As illustrated in Figure 1b, attack on the *endo* rotamer is favored over the *exo* by 1.5 kcal mol^{-1} if the *ipso* substituent is a hydrogen atom. But just as methyl substitution adds a bias favoring *exo* aldehyde rotamers in the ground-state structures, it also stabilizes the *exo* relative to the *endo* attack TS, leaving the two paths essentially equal in energy. Thus, *ipso* substitution is expected to both enhance the proportion of *exo* conformations and lower the barrier to attack on such forms, favoring product formation through the *AX* and *SX* forms. Herein, we will refer to the latter phenomenon as the ‘*ipso* effect’ during our discussions.

Chelation effects: Chelation of the organometallic’s metal center may drastically alter the conformational energy landscape by selectively favoring the *AN* conformation (the only conformation of the four that is able to support chelation between the nitrogen and the aldehyde) provided that *AN* is not too much higher in energy than the other rotamers. Meanwhile, the carbonyl polarization due to Lewis acid complexation further activates the carbonyl in this already reactive *endo* rotamer for *pro-syn* attack (Figure 2). Because of the intimate involvement of solvent and reagent aggregation, it is difficult for theory to directly compare energies of chelating and non-chelating paths on an equal footing. However, between the competing *pro-syn* and *pro-anti* chelating paths calculated for dimethyl zinc attack on **Me-H3** in CH_2Cl_2 (Figure 2), the *pro-syn* route is substantially favored, as its TS is closer to the ground state *AN* conformation with the CHO moiety bisecting the aziridine ring. In contrast, the CHO group in the *pro-anti* TS appears nearly perpendicular to either of the ground state bisecting conformers of the aldehyde. Noting that the aziridine–CHO rotational barrier in isolation is calculated to be 6 kcal mol^{-1} , this difference in

conformations represents a substantial extra energy cost for *pro-anti* attack. This finding concurs with the previously reported experiments and analysis by Pierre et al., in which CH_3Li and PhLi addition to *N*-*tert*-butyl-aziridine-2-carboxaldehyde showed a strong preference for *pro-syn* attack, despite the absence of any perturbing *cis* substituents.^[8] As the experiments below illustrate, specific chelation effects are easily revealed by simple competition with multidentate ligands, such as tetramethylethylenediamine (TMEDA).

Steric effects of *cis* substituents: It seems clear that a *cis* substituent (either the group on C3 or the nitrogen inveromer with the protecting group *syn* to the aldehyde) should hinder the approach of nucleophiles to the blocked face of the aldehyde carbonyl. However, such steric reasoning does not include the effects of polarity in the N protecting groups, which may interact with the carbonyl group’s dipole, orienting it and potentially modifying its reactivity. Such effects have been clearly observed in infrared studies focusing on the carbonyl group’s resonance as a probe of conformational preferences.^[21] Similarly, in the case of the Moc substituent in **Moc-trans**, the favorable electrostatic interaction between the aldehyde’s carbonyl oxygen and the Moc group’s electrophilic center plays a role akin to metal chelation of the aziridine nitrogen, inducing a substantial preference for the strongly *pro-syn*-selective *SN* conformation. The ‘electronically chelated’ Moc/aldehyde group (see Figure 6 below for an illustration of the aforementioned interaction) places the Moc substituent *syn* to the aldehyde, which is in contrast to the benzyl protected aziridines that necessarily have the protecting group *anti* to the aldehyde as a result of the chelating arrangement of the nitrogen lone pair and the carbonyl group. This orientation effect is also seen in a related X-ray crystal structure of Boc-protected aziridine **8** described below. In the analogous framework, but with the negatively polarized Ts group in **Ts-trans**, the aldehyde carbonyl orients away, weakly favoring the *SX* conformation. If that conformation is more strongly preferred, as in **Ts-2,3Di**, for which the *ipso* substituent exerts extra *exo* preference, the *SX* conformation dominates, the Ts group effectively blocks approach to the *pro-anti* face, and the resulting *pro-syn* addition yields exclusively *syn* products.

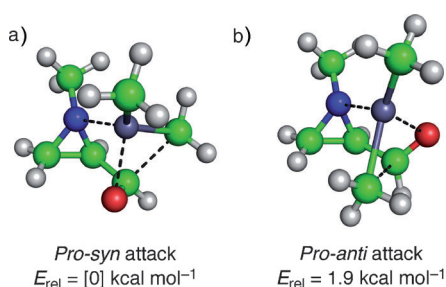
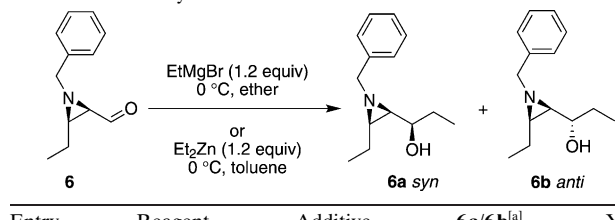


Figure 2. B3LYP/6-31+G*-optimized TS structures (relative energies) for chelation-controlled attack on the *AN* conformer of the model compound **Me-H3**. Notably, the *pro-anti* path (b) is calculated to be 1.9 kcal mol^{-1} higher in energy than the *pro-syn* path (a).

Bn-protected aziridine-2-carboxaldehydes: Addition of ethylmagnesium bromide to *N*-benzyl-*cis*-3-ethylaziridin-2-carboxaldehyde **6** (Table 3, entry 1) provided the *syn*^[22] adduct **6a** exclusively. The corresponding zinc reagent afforded a cleaner reaction with improved yield and similarly high *syn/anti* ratio (Table 3, entry 2). However, addition of TMEDA, a strong chelator of magnesium ions, lowered the *syn* selectivity (Table 3, entry 3). Thus, chelation of the organometallic compound’s metal center by the electron-rich nitrogen and the carbonyl oxygen appears to be the key to the selectivity of the reaction (Figure 3a). To avoid eclipsing steric interactions, the *N*-Bn substituent in the *cis*-substituted substrate is expected to prefer the *anti* conformation, with the

Table 3. Addition of organometallic reagents to Bn-protected *cis*-aziridine-2-carboxaldehydes.

Entry	Reagent	Additive	6a/6b ^[a]	Yield
1	EtMgBr	–	>99:1 ^[b]	75
2	Et ₂ Zn	–	>99:1 ^[b]	85
3	EtMgBr	TMEDA ^[c]	62:38	65

[a] Diastereomeric ratios were determined by NMR spectroscopy.

[b] Only the *syn* compound was observed by NMR spectroscopy.

[c] TMEDA (10 equiv) was used.

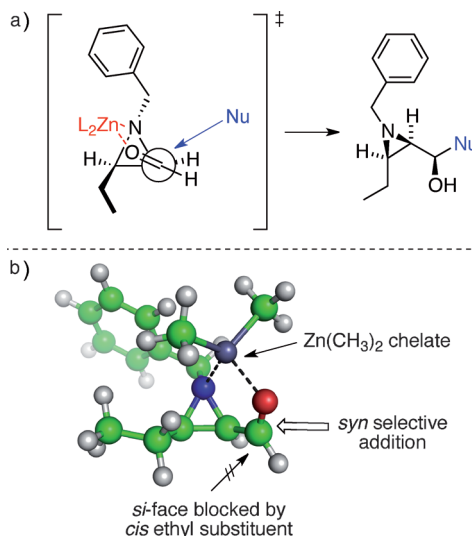


Figure 3. a) Proposed *syn*-selective attack on *N*-benzyl-*cis*-3-ethylaziridine-2-carboxaldehyde **6** under chelation control. b) RHF/3-21G-optimized structure of **6** chelating $Zn(CH_3)_2$. The structure rationalizes the observed high *syn* selectivity, as the *anti* approach is blocked by the *cis*-ethyl substituent.

nitrogen atom lone pair on the same face as the aldehyde (the *AN* conformation). This arrangement ideally sets the stage for chelation to control the aldehyde carbonyl group's orientation. In the resulting chelate, the *anti* approach should be blocked by the *cis* ethyl substituent leaving *syn* addition as the dominant pathway, consistent with the strong *syn* preference seen in these reactions (Figure 3b). It should be noted that chelation offsets the intrinsic preference for the *AX* conformer, which is favored by only $\approx 0.5 \text{ kcal mol}^{-1}$ in the model **Me-cis** system. This line of reasoning is exactly how Pierre et al. rationalized the strong stereoselectivity they observed for $LiAlH_4$ reductions of aziridinyl ketones in diethyl ether.^[8] Although the *cis* substituent clearly augments the observed selectivity,^[4a] it is not the only directing factor; even *N*-*tert*-butylaziridine-2-carboxaldehyde, with no additional substituents and the *tert*-butyl group oriented *trans* to the aldehyde, prefers the *syn*

reaction pathway with CH_3Li and $PhLi$, yielding products in *syn/anti* ratios of 4:1 and 2.5:1, respectively.^[8] In related work, Noh et al. reported a similar chelation-controlled strong preference for *syn* products in organometallic additions to an *N*-alkylated aziridine-2-carboxaldimine lacking any additional substituents on the ring.^[23] Similarly, Hou et al. have reported additions of phosphite ions to *N*-benzyl-2-aziridinesulfonimines; as expected for a chelation controlled process, more Lewis acidic metal ions favored *syn* selectivity, which plummeted when less coordinating ions, such as Na^+ , were used.^[24]

Added TMEDA destroys the reaction's selectivity, presumably by blocking chelation in the Grignard reaction of compound **6** (Table 3, entry 3). Thus, an uncomplexed neutral aldehyde apparently has little intrinsic selectivity. Computational modeling on **Me-cis**, the analogue of **6** used for computational analysis (see Table 1), shows a small energy difference between *endo*- and *exo*-CHO rotamers for the *anti* series (the *syn* series are not considered here since they are energetically inaccessible). Thus, an incoming nucleophile could react with either the *pro-syn* or *pro-anti* face of the aldehyde with nearly equal probability, even as it avoids the face shielded by the *cis* oriented ethyl group. Interestingly, despite the (presumably *anti*-selective) *AX* conformation being lower in energy (see Table 1) and thus prevalent, a 62:38 preference for *syn* addition is still seen; evidently the smaller population of *AN* outcompetes *AX*, supporting the notion that *endo* conformations are more reactive.

With chelation's observably important role in stereochemical control, it was natural to attempt a direct study of the chelating properties of the *N*-benzyl aziridine-2-carboxaldehydes by NMR spectroscopy. Unfortunately, the *cis* substituted *N*-benzyl aziridine-2-carboxaldehyde **6** uniformly formed precipitates when combined with $MgBr_2$, $MgCl_2$, or $ZnCl_2$ in $CDCl_3$ or $[D_8]toluene$. Evidently, association does occur with these Lewis acidic MX_2 species. However, in Grignard reactions of **6**, no precipitates were noted. Perhaps when the X (Cl or Br) on the metal is small and polar, the resulting complex is also polar enough to aggregate and precipitate, whereas with an organic group in place of a simple halide the complexes remain soluble.

In contrast to the *cis* case, *trans* aziridine carboxaldehyde **7** (Table 4) was found to exist as a mixture of two invertomers in a 1:1.2 ratio. Structural assignments based on 1H NMR spectroscopy (NOE analysis) suggest that the favored invertomer is *syn* with the benzyl and aldehyde substituents on the same side of the aziridine ring (e.g., structures *SX* or *SN* in Figure 4). This finding is in accord with conventional notions of steric demand that suggest the aldehyde should be smaller than the ethyl group (their respective A values are 0.56–0.8 and 1.79).^[25] Furthermore, for *trans*-1,3-dimethyl-2-acetyl aziridine, Pierre et al. found a 3:1 preference for the *syn* conformation.^[21] Also, the results stand in agreement with our DFT results for the model aziridine **Me-trans** in simulated CH_2Cl_2 , in which, for the respective *syn* and *anti* analogues of **7**, the *SN* conformer lies $0.3 \text{ kcal mol}^{-1}$ lower than *AN*. Perhaps even more important

Table 4. Addition of organometallic reagents to *Bn*-protected *trans*-aziridine-2-carboxaldehydes.^[a]

Entry	Reagent	Additive	<i>7a/7b</i> ^[b]		Yield
			55:45 ^[c]	55:45 ^[c]	
1	EtMgBr	—	55:45 ^[c]	55:45 ^[c]	75
2	EtMgBr	TMEDA ^[d]	55:45 ^[c]	55:45 ^[c]	85

[a] Exists as 55:45 mixture of invertomers at N observable by NMR spectroscopy at 25°C. [b] Diastereomeric ratios were determined by NMR spectroscopy. [c] The *syn* and *anti* compounds could not be separated. NMR analysis of the product mixtures showed a 55:45 mixture of unassigned stereoisomers. [d] TMEDA (10 equiv) was used.

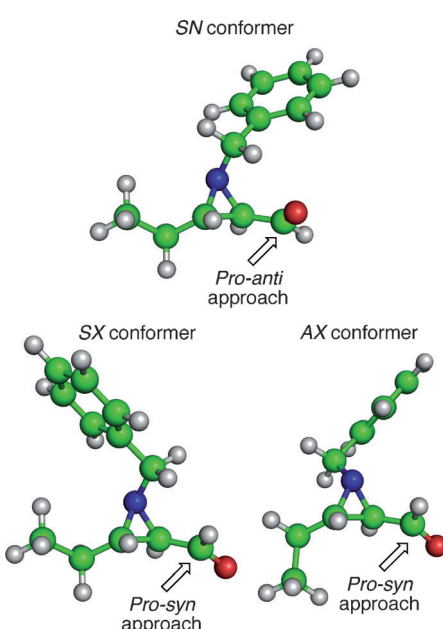


Figure 4. Energy-minimized conformers of *Bn*-protected *trans* substrate 7. Among these forms, both *pro-syn* and *pro-anti* faces are equally available. Of the **Me-trans** model structures, the *SX* and *AX* conformers lie only 0.3 kcal mol⁻¹ above the lowest energy *SN* form; B3LYP/6-31G*/SM8 energies of the actual structures space them more widely but still compress their overall energy range to \approx 1 kcal mol⁻¹. In contrast, the potentially chelating *AN* conformer lies an additional 1.3 kcal mol⁻¹ higher, which explains the apparent lack of chelation in additions to 7.

for the reaction's stereochemical outcome is the calculated energy difference between the model *endo* and *exo* aldehyde rotamers *SN* and *SX* (see Table 1), which for **Me-trans** is also quite small, suggesting little differentiation between access to the two faces of the aldehyde carbonyl. One might expect chelate formation to offer stereocontrol through the *AN* conformation of 7. However, upon addition of ethyl magnesium bromide to compound 7, an almost equimolar mixture of *syn* and *anti* adducts **7a** and **b** was obtained (Table 4, entry 1). Notably, this diastereomeric ratio was unaffected by addition of TMEDA (Table 4, entry 2); thus, it

appears that complexation is unimportant in reactions with this substrate. This finding makes sense in light of the high relative energy calculated for the *AN* conformer, a significant point of contrast with the chelation-capable *cis* substrate **6**. For **6**, chelation locks the carbonyl rotamer in the *AN* geometry, and the ethyl substituent offers strong stereo-differentiation by blocking one face of the aldehyde. We were thus surprised at first to find that, as with **6**, addition of Lewis acidic MX₂ to **7** quantitatively precipitated complexed aldehyde, removing it from solution in both toluene and chloroform; evidently, these systems are capable of strong monodentate complexation, a conclusion supported by the structural studies of Bartnik et al.^[26] Notably, in the X-ray crystal structure of a ZnBr₂ complex of 2-benzoyl aziridine, the heterocycle only serves as a monodentate ligand through nitrogen, despite the carbonyl group being in an *endo* conformation. This finding suggests that chelation in the aziridine-2-carbonyl framework is at most capable of modest energy lowering, on the same energy scale as conformational variations.

For substrate **7**, our analysis points to the *SN* conformation (Figure 4) as the lowest energy form. Here, a favorable dipole–dipole interaction between the *Bn*–N and aldehyde C=O moieties favors the *endo* orientation of the aldehyde carbonyl (Figure 5). This conformation itself would be ex-

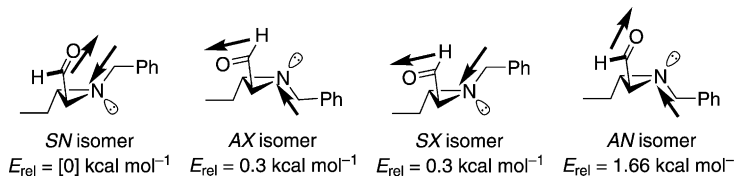


Figure 5. Dipole interactions between the *Bn*–N and CHO moieties in 7, proposed to explain the relative order of stability of the conformers. Relative energies shown are those calculated for the model system **Me-trans**. Based on the simple steric size order CHO < Et, the *syn* systems *SN* and *SX* should be favored. However, the added dipole repulsion in *AN* and attractions in *AX* and *SN* ultimately disfavor chelation in this system by pushing *AN* to a relatively high energy. Presumably, the sterically unfavorable *AX* isomer lies close in energy to *SX* as a result of *AX*'s favorable dipole interaction counterbalancing *SX*'s less than ideal dipole arrangement.

pected to have a modest *syn* preference, but the two low-lying *exo* forms (*SX* and *AX*) that are only a fraction of a kcal mol⁻¹ higher in energy offer reactivity favoring the *anti* product. This equilibrating mix of conformers explains the unselective addition reactions found both in the presence and absence of the TMEDA additive (Table 4, entry 2). Thus, for *N*-benzyl-protected *trans* substrates, almost no *de* is seen in the mixture of *syn* and *anti* adducts as neither chelation nor a single strong candidate among the free conformers is available to control the stereochemistry of the Grignard addition reaction.

Boc-protected aziridine-2-carboxaldehydes: In contrast to the *N*-benzyl cases discussed above, for which the *cis*-substi-

tuted system was most selective, in the *N*-Boc series, it is the *trans* substrates that show the greatest selectivity. Addition of methyl magnesium bromide to Boc-protected *trans*-3-cyclohexylaziridine-2-carboxaldehyde **8** led exclusively to the formation of *syn*^[27] alcohol **8a** (Table 5, entry 1). To our sur-

Table 5. Addition of organometallic reagents to Boc-protected *trans*-aziridine-2-carboxaldehydes.

Entry	Additive	8a / 8b ^[a]	Yield
1	–	>99:1 ^[b]	85
2	–	>99:1 ^[b,c]	83
3	TMEDA ^[d]	>99:1 ^[b]	80
4	MgBr ₂ ·OEt ₂ ^[e]	>99:1 ^[b]	78

[a] Diastereomeric ratios were determined by NMR spectroscopy.

[b] Only the *syn* compound was observed by NMR spectroscopy. [c] Reaction was carried out at –78°C. [d] TMEDA (10 equiv) was used. [e] Freshly prepared MgBr₂·OEt₂ (2.5 equiv) was used.

prise, despite the N activation expected from the Boc group, ring-opened products were not observed during these additions even near ambient temperatures; comparable yields and selectivities of product **8a** were obtained at 0°C and at –78°C (Table 5, entry 2). Addition of strong chelating reagents, such as TMEDA, or Lewis acids, such as MgBr₂·OEt₂, had no effect on the isomer distribution of the product; in fact, the *anti* addition compound **8b** was never seen to form under any of the reaction conditions studied, as confirmed through independent Mitsunobu conversion of **8a** into **8b** (see the Supporting Information) and spectroscopic analysis. Thus, in contrast to the *N*-benzyl series, for the *N*-Boc aziridine-2-carboxaldehydes, it is the *trans* substrates that show excellent *syn* selectivity in a non-chelation-controlled Grignard addition (Table 5, entries 3 and 4). This finding is at odds with a previous report^[4b] in which a chelate is suggested between the nitrogen lone pair, the aldehyde carbonyl oxygen and the magnesium atom. However, the observed failure of additives to alter the selectivity ratios argues against this scenario. Although the Boc group's carbonyl oxygen could offer a coordination site to participate in chelation, the unfavorable 7-membered-ring size and the Boc group's strong preference for conformations that maintain conjugation between the nitrogen lone pair and the Boc carbonyl group make chelation appear unlikely.

This issue is further illuminated by the X-ray crystal structure of Boc-protected *trans* substrate **8** (Figure 6a), in which the Boc and carboxaldehyde moieties are in the *SN* conformation. Interpretation of crystal structures as models for relevant solution state conformations of reactive species must be approached skeptically,^[28] due to crystal packing interactions and the absence of solvation effects. However, this relatively rigid and hydrophobic compound is only capable of modest dipole–dipole and van der Waals interactions in the

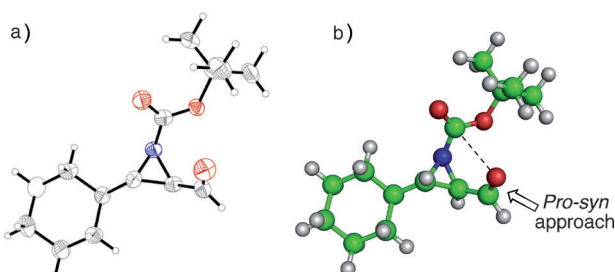


Figure 6. Comparison of the crystal structure of **8** (a) with its B3LYP energy minimized model (b) illustrates excellent similarity. Both structures indicate the *SN* isomer is the most stable conformation. The dotted line highlights the favorable electrostatic arrangement of the aldehyde with the Boc carbonyl (electrostatically chelated).

lattice, so its internal structural preferences would likely dominate the conformation that crystallizes. Also, for both the actual substrate **8** and, more rigorously, on our model system **Moc-trans**, calculations find a strong preference for the same conformation that is found in the X-ray crystal structure, as shown in Figure 6b. The contact distance (2.8 and 2.9 Å for X-ray and calculated structures, respectively) between the aldehyde oxygen and the Boc carbonyl carbon is substantially below that of a van der Waals contact (3.2 Å), suggesting a favorable interaction. This notion is reinforced by the observation of pyramidalization at the Boc carbon; the N–C=O–O torsion angle is compressed (172° experimental; 173° theory) from the expected 180°, suggesting the beginning of a Bürgi–Dunitz-like attack trajectory and the corresponding electrophilic activation of the aldehyde carbonyl.^[29] The effect of this aldehyde–Boc dipole–dipole attraction is to favor both the *endo* orientation of the aldehyde and the nitrogen invertomer with the Boc group *cis* to the aldehyde moiety, that is, the *SN* conformation. In a similar manner to the chelate structure invoked for addition to *cis*-Bn system **6**, this *SN* form favors attack on the more accessible and reactive *pro-syn* face of the aldehyde, yielding the observed high selectivity (compare Figures 3b and 6b to note similarities in conformation and the resulting face selectivity).

The case of Boc-protected *cis* aziridine-2-carboxaldehyde is less clear-cut than that of the *trans* compound in terms of selectivity; addition of Grignard reagents resulted in moderate yields with variable low to high *syn* selectivity (Table 6). Ring-opening products were frequently observed if the reaction was carried out at room temperature. As a result, Grignard additions were run at 0°C and then slowly warmed to room temperature. Notably, *syn* selectivity improved as the size of the nucleophile increased (compare Table 6, entries 1 vs. 5). Chelation appears to exert weak effects on this addition; formation of the Lewis acidic dialkyl zinc^[5a,30] reagent (Table 6, entry 3) led to a modest increase in *syn* selectivity, whereas addition of TMEDA decreased it (Table 6, entries 2 and 6). Simple steric arguments suggest that the Boc protecting group should be situated *trans* to the aziridine substituents. Our modeling studies agree, but find only small energy differences (0.1–0.5 kcal mol^{–1}) among the

Table 6. Addition of organometallic reagents to Boc-protected *cis*-aziridine-2-carboxaldehydes.

Entry	R	T [°C]	Additive	9a/9b ^[a]		Yield
				9a-C ₂ H <i>syn</i>	9a-Ph <i>syn</i>	
1	C ₂ H	0	—	59:41 ^[b]	—	53
2	C ₂ H	0	TMEDA ^[c]	50:50 ^[b]	—	51
3	C ₂ H	0	ZnCl ₂ ^[d]	70:30 ^[b]	—	60
4	C ₂ H	-78	—	52:48 ^[b]	—	50
5	Ph	0	—	90:10	—	55
6	Ph	0	TMEDA ^[c]	61:39	—	52
7	Ph	-78	—	88:12	—	49

[a] Diastereomeric ratios were determined by NMR spectroscopy. [b] Stereochemistry of the *anti* alcohol was confirmed by X-ray crystallography. [c] TMEDA (10 equiv) was used. [d] Anhydrous ZnCl₂ (2.5 equiv) was used.

AX, *AN*, and *SN* conformers for the **Moc-cis** model system. Although the *AX* conformer is lowest in energy, *AN* and *SN* are only 0.2–0.3 kcal mol⁻¹ higher in energy. Thus, two factors seem to be relevant in this system: 1) Weak chelation between the CHO and N groups in the *AN* conformer shifts the proportions of nearly equienergetic conformers towards those that favor the *syn* products. 2) Larger nucleophiles discriminate more strongly against *exo* conformers (*AX* in this case) than smaller nucleophiles, presumably owing to the *exo* rotamer being harder to attack, as discussed above (Figure 1b). Thus, the greater selectivity seen with the larger nucleophile suggests that the *endo* conformers *AN* and *SN* dominate those additions. Interestingly, the favorable dipole–dipole interaction between the aldehyde carbonyl and the Boc group appears to almost completely offset the steric effects of the *cis* hexyl side chain, placing the *SN* invertomer only 0.3 kcal mol⁻¹ above *AX* in the **Moc-cis** model, and 0.4 kcal mol⁻¹ higher in compound **9** itself. This last finding highlights the favorable aldehyde–Boc dipole–dipole interaction seen in the *trans* case to control both ground-state conformation and addition stereochemistry.

Formation of a cyclic chelate (Figure 7a) with the metal of methylmagnesium chloride coordinated between nitrogen and the aldehyde oxygen might explain the modest prefer-

ence for the *syn* addition product. However, although it remains pyramidalized due to being in a three-membered ring, the somewhat delocalized carbamate nitrogen would only be capable of weak binding at best, unlike in *N*-Bn *cis* substrate **6**, for which chelation is clearly the controlling factor. As a result, transition states based on the *AX* conformation of the aldehyde may compete; with the *cis* substituent blocking the approach from the *pro-syn* face, these conformations should lead to predominantly *anti* addition (Figure 7b). Thus the opposing effects of weakly chelation-favored *endo*, aldehyde–Boc attraction, and energetically close *exo* aldehyde orientations may explain the limited selectivity found in these additions.

In the case of Boc-protected 2,3-disubstituted aziridine-2-carboxaldehyde **10**, the reaction occurred with moderate to good *syn* selectivity. Both reactivity and conversion rates were found to diminish at lower temperatures, as seen with the *cis* substrates (Table 7, entries 3 and 4). Addition of

Table 7. Addition of organometallic reagents to Boc-protected 2,3-disubstituted aziridine-2-carboxaldehydes.

Entry	T [°C]	Additive	10a/10b ^[a]		Yield
			10a <i>syn</i>	10b <i>anti</i>	
1	0	—	85:15 ^[b]	—	85
2	0	TMEDA ^[d]	85:15 ^[b]	—	72
3	-78	—	60:40 ^[b]	—	51 ^[c]
4	-78	TMEDA ^[d]	71:29 ^[b]	—	48

[a] Diastereomeric ratios were determined by NMR spectroscopy. [b] Stereochemistry was determined as discussed in the Supporting Information; [c] Conversion=79%; for all other entries, conversion=100%. [d] TMEDA (10 equiv) was used.

TMEDA also showed temperature-dependent selectivity effects, enhancing *syn* adduct formation at -78°C (Table 7, entry 4) but not at 0°C (Table 7, entry 2). The calculated lowest energy conformation of **10** has both the Boc and the aldehyde on the same side of the ring, but between the competing effects of the alpha substituent, which favors the *exo* rotamer (Figure 8a), and the dipole–dipole interaction with the Boc group, which favors the *endo* rotamer (Figure 8b), there is little ground-state conformational preference.

The temperature effect disclosed in Table 7 seems counterintuitive. We speculate, however, that the higher *syn/anti* ratio at higher temperatures might be due to an increase in population of the highly *syn*-selective *SX* conformer. Based on the energetics of the **Moc-2,3Di** model system, the slightly lower energy *SN* isomer should predominate (Figure 8). However, if the *SX* isomer had both higher reactivity and stronger *syn* selectivity (as expected due to the shielding of the *pro-anti* approach by the Boc group), its contribution to product formation would grow quickly with increasing temperature. As noted earlier, *ipso* alkyl substitution enhances the reactivity of *exo* versus *endo* aldehyde rotamers; thus *SX* reactivity would be enhanced by the methyl substitution

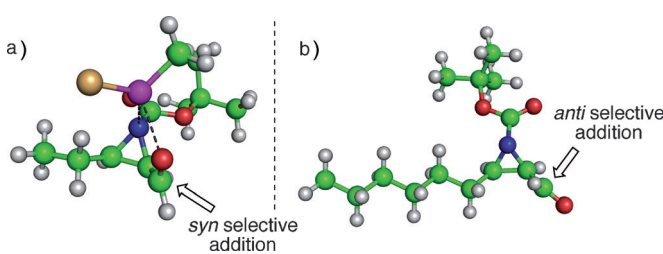


Figure 7. a) Chelated *AN* conformation of a model simulating Boc-protected *cis*-aziridine **9** would favor *syn*-selective addition (pictured with MeMgCl). b) The *exo* isomer (*AX*) is not capable of chelation and would favor a *pro-anti* approach of the nucleophile.

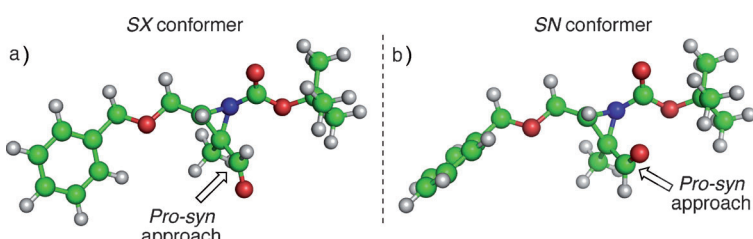
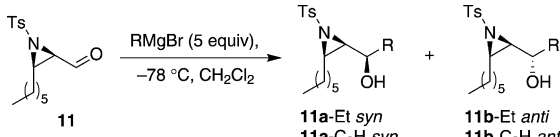


Figure 8. Low energy conformers of **10** showing near isoenergetic a) SX ($0.23 \text{ kcal mol}^{-1}$) and b) SN (0 kcal mol^{-1}) CHO rotamers [note: these energies are for the **Moc-2,3Di** modeled SX and SN isomers].

at the *ipso* position (see discussion of the *ipso* effect above). At -78°C , the less *syn* selective *SN* isomer would dominate due to both the decreased temperature and potentially due to Lewis acid amplification of the Boc group's pseudochelating interaction with the aldehyde.^[31] The latter notion is further supported by the results for TMEDA addition at -78°C , which increases the *syn/anti* product ratio, presumably by disrupting the proposed *SN*-supporting complexation.

Ts-protected aziridine-2-carboxaldehydes: Grignard addition to Ts-protected *cis*-aziridine-2-carboxaldehydes was accompanied by undesired nucleophilic aziridine ring opening. To suppress these reactions, it was crucial to carry out the addition at -78°C . The *cis* substrate **11** exhibited poor reactivity towards nucleophilic addition at the aldehyde carbonyl at this temperature. Conversion was low even after adding an excess (10 equiv) of the Grignard reagent. In all cases, the desired alcohol was either difficult to isolate, or if isolable, was recovered in low yield (Table 8, entry 2).

Table 8. Addition of organometallic reagents to Ts-protected *cis*-aziridine-2-carboxaldehydes.



Entry	R	Additive	11a/11b ^[a]	Yield
1	Et	—	50:50	n.d. ^[b]
2	C ₂ H	—	56:43	20
3	C ₂ H	TMEDA ^[c]	50:50	n.d. ^[b]
4	C ₂ H	MgBr ₂ •OEt ₂ ^[d]	50:50	85

[a] Diastereomeric ratios were determined by NMR spectroscopy.

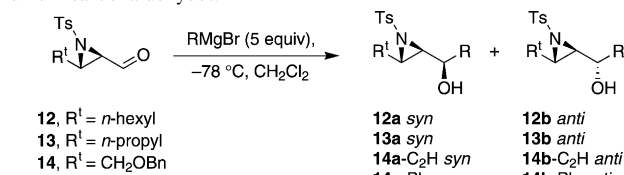
[b] Yields could not be determined due to undesired side reaction products. [c] TMEDA (10 equiv) was used. [d] Freshly prepared MgBr₂•OEt₂ (2.5 equiv) was used.

In an attempt to promote the reaction by Lewis acid activation, MgBr₂•OEt₂ was added. In this case, higher yields of the alcohol products were isolated (Table 8, entry 4), but no higher selectivity between the *syn* and *anti* adducts was observed than in the other cases. The product ratios were not altered under chelating or non-chelating conditions, which argues against the involvement of a chelated transition state. As observed with the Bn-protected *cis*-aziridine-2-carboxal-

dehydes, only one invertomer needs to be considered, since the protecting group is situated *trans* to the substituent. Although the calculated lowest energy conformation is *exo*, multiple *exo* and *endo* conformations lie within $0.5 \text{ kcal mol}^{-1}$ of the lowest form, differing only in the rotameric orientations of the ethyl and tosyl groups. Thus both faces of the carbonyl are expected to be equally prone to nucleophilic attack, which explains the lack of diastereoselectivity.

Addition of Grignard reagents to *trans*-substituted *N*-Ts aziridine-2-carboxaldehydes proceeded with moderate to excellent *syn* selectivity and good yields (Table 9, entries 1–7). In this case, nucleophilic ring-opening reactions were completely suppressed at -78°C . Chelation appears to play no role in these reactions as addition of MgBr₂•OEt₂ (Table 9, entry 3) or TMEDA (Table 9, entry 2) had no remarkable effect either on selectivity or yield.

Table 9. Addition of organometallic reagents to Ts-protected *trans*-aziridine-2-carboxaldehydes.



Entry	Substrate	R	Additive	a/b ^[a]	Yield
1	12	C ₂ H	—	70:30	76
2	12	C ₂ H	TMEDA ^[b]	70:30	73
3	12	C ₂ H	MgBr ₂ •OEt ₂ ^[c]	69:31	75
4	13	C ₂ H	—	70:30	81
5	13	C ₂ H	MgBr ₂ •OEt ₂ ^[c]	72:28	69
6	14	C ₂ H	—	67:33	71
7	14	Ph	—	>99:1	85

[a] Diastereomeric ratios were determined by NMR spectroscopy.

[b] TMEDA (10 equiv) was used. [c] Freshly prepared MgBr₂•OEt₂ (2.5 equiv) was used.

In the calculated minimum energy conformation of **13** (Figure 9), the aldehyde moiety has a strong preference for the *exo* orientation. The **Ms-trans** model indicates that the *SX* isomer is $0.5 \text{ kcal mol}^{-1}$ more stable than the *AX* isomer. As such, the bulky tosyl group in the *SX* isomer blocks one face of the carbonyl and directs the nucleophile to approach from the opposite direction, yielding the *syn* addition product. On the other hand, the *AX* isomer is less *syn* selective, owing to the fact that the Ts group is on the opposite face of the aziridine ring. This is presumably the cause of the lowered overall *syn/anti* product ratios. With this in mind, we hypothesized that increasing the size of the incoming nucleophile would increase the stereodifferentiation since the *pro-anti* approach of the *AX* isomer would be sterically re-

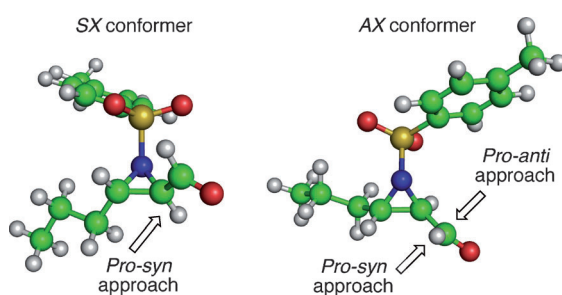


Figure 9. The lower energy *SX* conformation of **13** is *syn* selective due to steric blocking afforded by the Ts protecting group. The *AX* conformer exhibits less steric bias and thus would reduce the overall stereoselectivity. The modest selectivity in Ts-protected *trans*-aziridine-2-carboxaldehyde could arise from the energetically close *SX* and *AX* conformers.

tarded. Indeed, addition of phenyl magnesium bromide to substrate **14** afforded exclusively the *syn* adduct **14a-Ph** in good yield (Table 9, entry 7).

Both high yield and exceptional *syn* selectivity were achieved with 2,3-disubstituted aziridine-2-carboxaldehyde **15** (Table 10). Similar to the *trans* system, selectivity was not at

Table 10. Addition of organometallic reagents to Ts-protected 2,3-disubstituted aziridine-2-carboxaldehyde.

Entry	R	Additive	a:b ^[a]	Yield
			15a-C₂H <i>syn</i> 15a-Ph <i>syn</i>	
1	C ₂ H	—	>99:1 ^[b,c]	92
2	C ₂ H	MgBr ₂ ·OEt ₂ ^[d]	>99:1 ^[b,c]	81
3	C ₂ H	TMEDA ^[e]	>99:1 ^[b,c]	79
4	Ph	—	>99:1 ^[b,c]	85

[a] Diastereomeric ratios were determined by NMR spectroscopy. [b] Only the *syn* isomer was seen by NMR spectroscopy. [c] Stereochemistry was confirmed by X-ray crystallographic analysis. [d] Freshly prepared MgBr₂·OEt₂ (2.5 equiv) was used. [e] TMEDA (10 equiv) was used.

all affected by addition of TMEDA (Table 10, entry 3) or MgBr₂·OEt₂ (Table 10, entry 2). As in the *trans* case, the energy-minimized conformation (Figure 10a) orients the aldehyde carbonyl *exo*, such that the tosyl group blocks the *pro-anti* face of the carbonyl, thus favoring *syn*-selective approach of the nucleophile. Based on the **Ms-2,3Di** model, the *SX* isomer is by far the most stable conformation. The high *exo* tendency is not only due to the Ts protecting group, but also, as described above, the result of the *ipso* methyl substitution. The highly favored *syn* orientation, as expected, originates from the nitrogen atom adopting the necessary invertomer to avoid a steric clash with the two substituents on the *anti* face of the aziridine ring. The crystal structure obtained for aziridine-2-carboxaldehyde **15** (Figure 10b) is in close agreement with our optimized structures, supporting the above rationalization of this substrate's

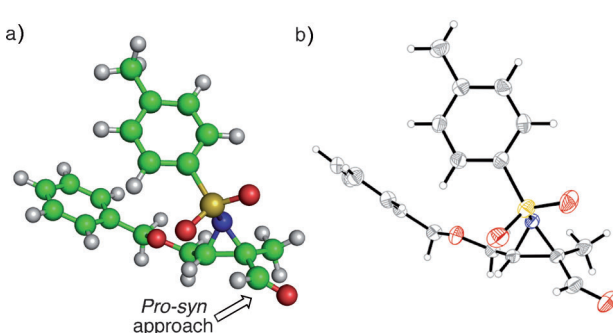
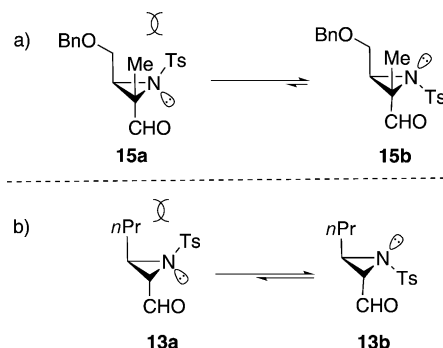


Figure 10. Comparison of the molecular structure of **15**, as determined by X-ray diffraction (b), with the lowest energy B3LYP/6-31G* optimized aziridine conformation (a) of **15**. The **Ts-2,3Di** model structure shows an analogous *SX*-type lowest conformation.

strong conformational preference and reaction stereoselectivity.

The structural similarity between the most stable ground-state conformations calculated for *trans* aziridines **12–14** and 2,3-disubstituted aziridine-2-carboxaldehyde **15** does not entirely justify the exceptional *syn* selectivity observed in the case of the 2,3-disubstituted aziridine-2-carboxaldehyde. The extra methyl substituent at the alpha position clearly makes a considerable difference in yield and level of stereoselectivity. A careful analysis of energy-minimized conformations for **13** and **15** suggests that the difference in stereoselectivity is a result of two factors, both of which favor a more defined ground-state conformation in **15** as compared to **13**. These factors are that 1) the tosyl group is sterically limited to a *syn* relationship with the aldehyde by the two alkyl substituents on the opposite ring face; and 2) the methyl group alpha to the aldehyde favors the *exo* aldehyde rotamer. Scheme 4 illustrates the expected invertomer equilibria for **13** and **15**, based on the energies calculated for the *syn* and *anti* (specifically, *SX* and *AX*) conformations of model compounds **Ms-trans** and **Ms-2,3Di**, respectively. As expected, the *syn* invertomers are favored in both cases, but the *AX*–*SX* ΔG energy difference is significantly larger (4.03 vs. 0.50 kcal mol⁻¹; see Table 1) for **Ms-2,3Di** than for **Ms-trans**, and hence by analogy for **15** than for **13**.



Scheme 4. a) The N invertomers of Ts-protected 2,3-disubstituted aziridine-2-carboxaldehyde. b) The N invertomers of Ts-protected *trans* aziridine aldehyde.

Although the steric bias toward *syn* (Scheme 4a) in **15** is straightforward, that in **13** results from a delicate balance between *n*-alkyl and CHO groups as substituents *cis* to the Ts group. The 0.50 kcal mol⁻¹ calculated *anti/syn* energy difference for **Ms-trans** predicts an invertomer ratio of 2.3:1 at 23°C. Because the barrier to nitrogen inversion is higher in aziridines than in other pyramidal nitrogen heterocycles, their invertomer spectra can readily be resolved in low-temperature NMR studies.^[32] We therefore resorted to dynamic ¹H NMR measurements to explore the conformational behavior of the *trans* and 2,3-disubstituted aziridine-2-carboxaldehydes **13** and **15** at different temperatures (Figure 11). In the case of **15**, resonances displayed essentially identical line shapes at temperatures from 25 to -70°C, confirming the exclusive presence of one conformation (presumably **15b** in Scheme 4a), which is expected (see Figure 11a vs. b

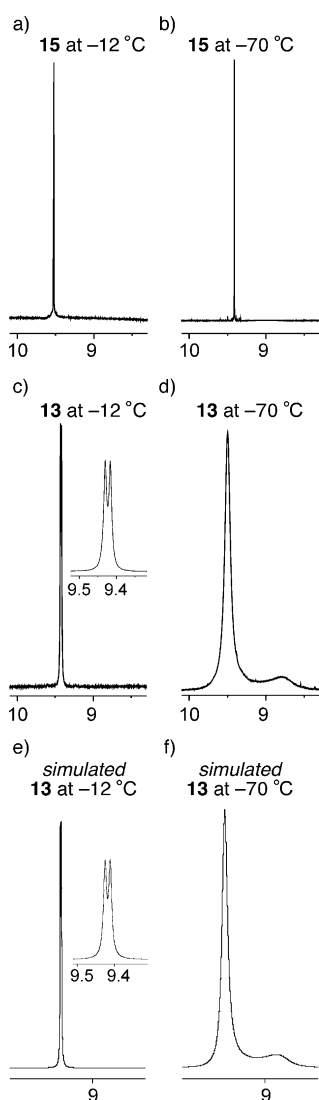


Figure 11. Aldehyde resonance of **15** at a) -12°C and b) -70°C. Aldehyde resonance of **13** at c) -12°C (expansion shown in the inset) and d) -70°C. e) Simulated aldehyde resonance of **13** at -12°C (expansion shown in the inset). f) Simulated aldehyde resonance of **13** at -70°C.

for NMR spectra). In contrast, compound **13** showed broadening of most peaks as a function of lowering temperature (Figure 11c vs. d). Of particular interest is the aldehyde resonance, which showed considerable broadening upon cooling and eventually exhibited decoalescence below -64°C. At the lowest temperature observed, -70°C, two distinct broad peaks were visible in a ratio of 88:12 (integrated ratio); this translates into a $\Delta\Delta G^\ddagger$ of 0.80 kcal mol⁻¹. Confirming the **Ms-trans** model system's calculated 0.58 kcal mol⁻¹ free-energy difference, a detailed conformational search and optimization of **13** at the B3LYP/6-31G* level with single-point SM8 "CH₂Cl₂" solvation calculations yielded a calculated $\Delta\Delta E$ of 0.63 kcal mol⁻¹ between the invertomers **13-SX** and **13-AX**; the resulting prediction of a 4.8:1 invertomer ratio is in reasonably good agreement with the \approx 7:1 value observed. Full line-shape analysis of the aldehyde resonance (Figure 11e and f),^[33] used to determine the activation parameters, leads to the calculation of the energy barrier for nitrogen inversion of **13** ($\Delta G^\ddagger = 10.7 \pm 1.4$ kcal mol⁻¹, $\Delta H^\ddagger = 7.99 \pm 0.3$ kcal mol⁻¹, and $\Delta S^\ddagger = -8.94 \pm 0.3$ cal mol⁻¹ K⁻¹, data from an Eyring plot, see the Supporting Information). The corresponding B3LYP/6-31G*/SM8-CH₂Cl₂ calculation for **Ms-trans** finds an inversion ΔG^\ddagger of 10.2 kcal mol⁻¹, quite similar to the experimental value for **13**.^[34] With this modest inversion barrier, both invertomers would be available throughout the reaction with the organometallic nucleophile. Presumably, this mix of substrate conformers also leads to the observed moderate selectivity in the addition of organometallic reagents to Ts-protected *trans*-aziridine-2-carboxaldehyde **13**, in contrast to the exclusive *syn* selectivity seen with SX-dominated 2,3-disubstituted aziridine-2-carboxaldehyde **15**.

Conclusion

The selectivity of organometallic addition to N-protected *cis*, *trans*, and 2,3-disubstituted aziridine-2-carboxaldehydes is governed by multiple intimately coupled factors. Most important are the rotameric orientation of the aldehyde functionality and invertomeric preference of the nitrogen protecting group. As with cyclopropane carboxaldehydes, the CHO moiety strongly prefers bifurcated geometries relative to the ring, with the oxygen oriented either *endo* or *exo*; rotation to other orientations can cost as much as 6 kcal mol⁻¹. Also, although conjugation might have been expected to oppose it, the aziridine nitrogen remains strongly pyramidalized regardless of which substituent it carries; invertomeric alternative conformations therefore must be considered. These aspects are further modulated by the N substituents' electronic nature, and by the steric environment set by the other substituents on the aziridine ring (see Table 11 for a summary). Additional variation arises from the use of different metal and alkyl components of the organometallic nucleophiles.

For Bn protected aziridine carboxaldehydes, selectivity originates from chelation, consistent with findings in the lit-

Table 11. Summarized results of the selectivity (*syn/anti*) observed in the addition reactions of organometallic reagents to aziridine carboxaldehydes.

Substitution pattern	<i>N</i> protecting group (R)		
	Bn	Boc	Ts
<i>cis</i>	excellent	poor	poor
<i>trans</i>	poor	excellent	moderate
2,3Di	—	moderate	excellent

erature. Excellent *syn* selectivity (>99:1 *syn/anti*) is achieved for *N*-Bn *cis* aziridine carboxaldehydes, whereas the *trans* substrates undergo almost completely unselective (55:45 *syn/anti*) addition. For this case, as well as the *N*-Boc-protected *cis* and 2,3-disubstituted systems, the low selectivity seems to be due to the substrates' conformational ambiguity, both between the aldehyde *endo/exo* rotamer and N invertomer structures. However, for the conformationally well-defined *N*-Boc *trans* substrates, extremely high *syn* selectivity (>99:1 *syn/anti*) is observed that is unaffected by chelation modifiers. This strong stereopreference appears to be dictated by the favorable chelation-like interaction between the aldehyde carbonyl and the *syn*-Boc group's electrophilic carbon. Because of amide resonance, the Boc substituent adopts a tangential rotameric orientation relative to the aziridine three-membered ring; this is the opposite of the bifurcated geometry preferred by the C-bonded aldehyde, and leads to their meshing in this complementary manner, causing mild Lewis acid activation of the aldehyde specifically in the *SN* conformation. For the *N*-Ts protected series, diastereoselectivity is again largely understandable in terms of the systems' conformational preferences. Although *cis* substrates do not enjoy any kind of selectivity, their *trans* analogues afford the addition product with moderate to high *syn* (70:30 *syn/anti*) selectivity, and exceptional stereospecificity is achieved in the case of *N*-Ts-2,3-disubstituted aziridine-2-carboxaldehyde **15** (>99:1 *syn/anti*). In the *trans* case, the *SX* (i.e., *syn* N invertomer and *exo* aldehyde rotamer) conformer dominates, but only weakly; in the 2,3-disubstituted case, the additional methyl substituent alpha to the carbonyl more definitively locks the *SX* conformer, enforcing *syn*-selective addition by attack on the aldehyde face away from the Ts group.

Thus, extremely high *syn* selectivity can be achieved with *cis* substrates utilizing Bn, *trans* substrates utilizing Boc, and 2,3-disubstituted aziridine-2-carboxaldehyde substrates bearing Ts as the nitrogen protective groups. The corresponding *anti* adducts can easily be accessed by Mitsunobu inversion, or by complementary hydride reduction of the related ketones, guided by the early conformational and synthetic analyses of Pierre et al., augmented by the more detailed conformational insights developed here with the aid of quantum chemical modeling.

Acknowledgements

Generous support was provided by the NIH (No. R01-GM082961). The authors are thankful to Dr. Daniel C. Whitehead for fruitful and illuminating discussions.

- [1] a) G. Cardillo, L. Gentilucci, A. Tolomelli, *Aldrichimica Acta* **2003**, *36*, 39–50; b) V. H. Dahanukar, I. A. Zavialov, *Curr. Opin. Drug Discovery Dev.* **2002**, *5*, 918–927; c) D. Tanner, *Angew. Chem.* **1994**, *106*, 625–646; *Angew. Chem. Int. Ed. Engl.* **1994**, *33*, 599–619; d) A. H. Li, L. X. Dai, V. K. Aggarwal, *Chem. Rev.* **1997**, *97*, 2341–2372; e) W. McCoull, F. A. Davis, *Synthesis* **2000**, 1347–1365; f) J. B. Sweeney, *Chem. Soc. Rev.* **2002**, *31*, 247–258.
- [2] a) J. C. Antilla, W. D. Wulff, *J. Am. Chem. Soc.* **1999**, *121*, 5099–5100; b) J. C. Antilla, W. D. Wulff, *Angew. Chem.* **2000**, *112*, 4692–4695; *Angew. Chem. Int. Ed.* **2000**, *39*, 4518–4521; c) T. B. Bisol, M. M. Sa, *Quim. Nova* **2007**, *30*, 106–115; d) C. A. Olsen, H. Franzyk, J. W. Jaroszewski, *Eur. J. Org. Chem.* **2007**, 1717–1724; e) H. M. I. Osborn, J. Sweeney, *Tetrahedron: Asymmetry* **1997**, *8*, 1693–1715; f) J. Vesely, I. Ibrahem, G. L. Zhao, R. Rios, A. Cordonova, *Angew. Chem.* **2007**, *119*, 792–795; *Angew. Chem. Int. Ed.* **2007**, *46*, 778–781; g) A. A. Desai, W. D. Wulff, *J. Am. Chem. Soc.* **2010**, *132*, 13100–13103.
- [3] J. M. Schomaker, A. R. Geiser, R. Huang, B. Borhan, *J. Am. Chem. Soc.* **2007**, *129*, 3794–3795.
- [4] a) J. Andres, N. de Elena, R. Pedrosa, A. Perez-Encabo, *Tetrahedron* **1999**, *55*, 14137–14144; b) G. Righi, S. Pietrantonio, C. Bonini, *Tetrahedron* **2001**, *57*, 10039–10046; c) G. Righi, S. Ciambrone, *Tetrahedron Lett.* **2004**, *45*, 2103–2106.
- [5] a) R. Noyori, M. Kitamura, *Angew. Chem.* **1991**, *103*, 34–55; *Angew. Chem. Int. Ed. Engl.* **1991**, *30*, 49–69; b) H. Urabe, O. O. Evin, F. Sato, *J. Org. Chem.* **1995**, *60*, 2660–2661; c) M. T. Reetz, *Angew. Chem.* **1984**, *96*, 542–555; *Angew. Chem. Int. Ed. Engl.* **1984**, *23*, 556–569.
- [6] a) N. Anh, *Top. Curr. Chem.* **1980**, *88*, 145–162; b) G. Righi, S. Ronconi, C. Bonini, *Eur. J. Org. Chem.* **2002**, 1573–1577; c) H. Urabe, F. Sato, *J. Org. Chem. Jpn.* **1993**, *51*, 14.
- [7] a) B. C. Kim, W. K. Lee, *Tetrahedron* **1996**, *52*, 12117–12124; b) C. S. Park, H. G. Choi, H. Lee, W. K. Lee, H.-J. Ha, *Tetrahedron: Asymmetry* **2000**, *11*, 3283–3292.
- [8] J. L. Pierre, H. Handel, P. Baret, *Tetrahedron* **1974**, *30*, 3213–3223.
- [9] a) Spartan '08, Wavefunction, Irvine; b) Y. Shao, L. F. Molnar, Y. Jung, J. Kussmann, C. Ochsenfeld, S. T. Brown, A. T. B. Gilbert, L. V. Slipchenko, S. V. Levchenko, D. P. O'Neill, R. A. DiStasio, R. C. Lochan, T. Wang, G. J. O. Beran, N. A. Besley, J. M. Herbert, C. Y. Lin, T. Van Voorhis, S. H. Chien, A. Sodt, R. P. Steele, V. A. Rassolov, P. E. Maslen, P. P. Korambath, R. D. Adamson, B. Austin, J. Baker, E. F. C. Byrd, H. Dachs, R. J. Doerksen, A. Dreuw, B. D. Dunietz, A. D. Dutoi, T. R. Furlani, S. R. Gwaltney, A. Heyden, S. Hirata, C. P. Hsu, G. Kedziora, R. Z. Khaliulin, P. Klunzinger, A. M. Lee, M. S. Lee, W. Liang, I. Lotan, N. Nair, B. Peters, E. I. Proynov, P. A. Pieniazek, Y. M. Rhee, J. Ritchie, E. Rosta, C. D. Sherrill, A. C. Simmonett, J. E. Subotnik, H. L. Woodcock, W. Zhang, A. T. Bell, A. K. Chakraborty, D. M. Chipman, F. J. Keil, A. Warshel, W. J. Hehre, H. F. Schaefer, J. Kong, A. I. Krylov, P. M. W. Gill, M. Head-Gordon, *Phys. Chem. Chem. Phys.* **2006**, *8*, 3172–3191.
- [10] A. D. Becke, *J. Chem. Phys.* **1993**, *98*, 1372–1377.
- [11] P. C. Hariharan, J. A. Pople, *Theor. Chim. Acta* **1973**, *28*, 213–222.
- [12] A. V. Marenich, R. M. Olson, C. P. Kelly, C. J. Cramer, D. G. Truhlar, *J. Chem. Theory Comput.* **2007**, *3*, 2011–2033.
- [13] L. A. Curtiss, P. C. Redfern, K. Raghavachari, V. Rassolov, J. A. Pople, *J. Chem. Phys.* **1999**, *110*, 4703–4709.
- [14] a) M. J. Aroney, K. E. Calderbank, H. J. Stootman, *J. Chem. Soc. Perkin Trans. 2* **1973**, 1365–1368; b) M. Pelissier, A. Serafini, J. Devanneaux, J. F. Labarre, J. F. Tocanne, *Tetrahedron* **1971**, *27*, 3271–3284; c) A. D. Walsh, *Nature* **1947**, *159*, 712–713.

[15] These structural and electronic issues will be explored in detail in a future manuscript.

[16] a) P. H. M. Delanghe, M. Lautens, *Tetrahedron Lett.* **1994**, *35*, 9513–9516; b) Y. Kazuta, H. Abe, T. Yamamoto, A. Matsuda, S. Shuto, *Tetrahedron* **2004**, *60*, 6689–6703; c) C. Mioskowski, S. Manna, J. R. Falck, *Tetrahedron Lett.* **1983**, *24*, 5521–5524; d) S. Ono, S. Shuto, A. Matsuda, *Tetrahedron Lett.* **1996**, *37*, 221–224.

[17] Y. Kazuta, H. Abe, A. Matsuda, S. Shuto, *J. Org. Chem.* **2004**, *69*, 9143–9150.

[18] J. L. Pierre, H. Handel, P. Baret, *Org. Mag. Res.* **1972**, *4*, 703–707.

[19] H. Handel, P. Baret, J. L. Pierre, *C. R. Acad. Sci. C Chim.* **1973**, *276*, 511–514.

[20] J. R. Durig, S. Y. Shen, *Spectrochim. Acta A Mol. Biomol. Spectrosc.* **2000**, *56*, 2545–2561.

[21] R. Barlet, P. Baret, H. Handel, J. L. Pierre, *Spectrochim. Acta Part A Mol. Spectrosc.* **1974**, *30*, 1471–1485.

[22] All of the spectroscopic data of the isolated compound **6a** matches with the *syn* addition product, as reported previously in the literature, see: Ref. [4a].

[23] H.-Y. Noh, S.-W. Kim, S. I. Paek, H.-J. Ha, H. Yun, W. K. Lee, *Tetrahedron* **2005**, *61*, 9281–9290.

[24] B.-F. Li, M.-J. Zhang, X.-L. Hou, L.-X. Dai, *J. Org. Chem.* **2002**, *67*, 2902–2906.

[25] E. L. Eliel, S. H. Wilen, M. P. Doyle, *Basic Organic Stereochemistry*, Wiley-Interscience, New York, **2001**.

[26] R. Bartnix, S. Lesniak, A. Laurent, *Tetrahedron Lett.* **1981**, *22*, 4811–4812.

[27] The spectroscopic data of the alcohol matches that of the *syn* compound reported by Righi and co-workers in their previous study, see: Ref. [4b].

[28] H. Kessler, G. Zimmermann, H. Forster, J. Engel, G. Oepen, W. S. Sheldrick, *Angew. Chem.* **1981**, *93*, 1085–1086; *Angew. Chem. Int. Ed. Engl.* **1981**, *20*, 1053–1055.

[29] H. B. Buergi, J. D. Dunitz, *Acc. Chem. Res.* **1983**, *16*, 153–161.

[30] M. Bhupathy, T. Cohen, *Tetrahedron Lett.* **1985**, *26*, 2619–2622.

[31] Chelation of the Boc carbonyl with divalent magnesium has been invoked previously in a number of publications; for an example, see: P. Merino, A. Lanasa, F. L. Merchan, M. Tejero, *Tetrahedron Lett.* **1997**, *38*, 1813–1816. To our knowledge these authors have not reported confirmatory experiments by using, for example, TMEDA or other complexants to address the chelation possibility.

[32] a) F. A. L. Anet, R. D. Trepka, D. J. Cram, *J. Am. Chem. Soc.* **1967**, *89*, 357–362; b) H. Kessler, *Angew. Chem.* **1970**, *82*, 237–253; *Angew. Chem. Int. Ed. Engl.* **1970**, *9*, 219–235; c) E. R. Johnston, *Mag. Res. Chem.* **1995**, *33*, 664–668; d) H. Nakanishi, O. Yamamoto, *Tetrahedron* **1974**, *30*, 2115–2121; e) J. D. Andose, J. M. Lehn, K. Mislow, J. Wagner, *J. Am. Chem. Soc.* **1970**, *92*, 4050–4056; f) S. J. Brois, *J. Am. Chem. Soc.* **1967**, *89*, 4242–4243; g) J. B. Lambert, B. S. Packard, W. L. Oliver, *J. Org. Chem.* **1971**, *36*, 1309–1310; h) H. A. Dabbagh, A. R. Modarresi-Alam, *J. Chem. Res.* **2000**, *2000*, 190–192.

[33] P. H. M. Budzelaar, gNMR 5.0.6.0, NMR Simulation Program, IvorySoft, **2006**.

[34] The calculated Gibbs energy of activation is a measure of all processes that contribute to the observed line broadening of the aldehyde resonances and, thus, is not solely a measure of the nitrogen inversion. In fact, it is anticipated that rotation about the C3–CO bond in **13** contributes to the calculated barrier.

Received: April 16, 2011

Published online: September 16, 2011